Clinical Imaging 56 (2019) 93–101

Contents lists available at ScienceDirect

Clinical Imaging

journal homepage: www.elsevier.com/locate/clinimag

Cardiothoracic Imaging

Impact of the sampling rate of dynamic myocardial computed tomography perfusion on the quantitative assessment of myocardial blood flow

Takahiro Yokoi[a], Yuki Tanabe[a], Teruhito Kido[a,*], Akira Kurata[a], Tomoyuki Kido[a], Teruyoshi Uetani[b], Shuntaro Ikeda[b], Hironori Izutani[c], Masao Miyagawa[a], Teruhito Mochizuki[a]

[a] Department of Radiology, Ehime University Graduate School of Medicine, Toon, Ehime, Japan
[b] Department of Cardiology, Pulmonology, Hypertension and Nephrology, Ehime University Graduate School of Medicine, Toon, Ehime, Japan
[c] Department of Cardiovascular and Thoracic Surgery, Ehime University Graduate School of Medicine, Toon, Ehime, Japan

ARTICLE INFO

Keywords:
Coronary artery disease
Dynamic computed tomography perfusion
Myocardial blood flow
Myocardial perfusion abnormality
Quantitative assessment

ABSTRACT

Background: The relationship between shot-to-shot sampling rates for dynamic myocardial computed tomography perfusion (CTP) and robustness of CTP-derived myocardial blood flow (CT-MBF) is debatable. We retrospectively investigated the influence of a reduced sampling rate for dynamic CTP on CT-MBF computation and diagnostic performance for detecting myocardial perfusion abnormalities.

Methods: Pharmacological stress dynamic whole-heart CTP was performed in 120 patients suspected with coronary artery disease. Dynamic CTP data were obtained for 30 continuous heartbeats during the R-peak to R-peak (1RR) interval on electrocardiography. Three additional datasets were created with sub-sampling acquisitions every 2, 3, and 4 heartbeats from the original dataset as interval times of 2RR, 3RR, and 4RR, respectively. CT-MBF was calculated using deconvolution analysis and determined as the mean value of the whole heart (global CT-MBF) and using the 16-segment model (segmental CT-MBF). The diagnostic performance of segmental CT-MBF for detecting perfusion abnormalities was compared to that of cardiac magnetic resonance imaging as the gold standard in 32 of 120 patients. These results were compared among the four CTP datasets.

Results: Global CT-MBFs for 1RR, 2RR, 3RR, and 4RR sampling were 1.57 ± 0.34, 1.54 ± 0.36, 1.51 ± 0.37, and 1.41 ± 0.33 mL/g/min, respectively. Areas under the receiver operating characteristic curves of segmental CT-MBF for 1RR, 2RR, 3RR, and 4RR sampling were 0.84, 0.83, 0.79, and 0.76, respectively (1RR versus [vs.] 2RR, non-significant; 1RR vs. 3RR or 4RR, $p < 0.05$).

Conclusion: CT-MBF with 2RR sampling has similar performance with regard to quantification and detecting myocardial perfusion abnormalities as that with 1RR sampling.

1. Introduction

Functional assessment of myocardial perfusion in patients with coronary artery disease (CAD) is important to help guide appropriate treatment strategies and determine prognosis [1,2]. Although non-invasive coronary computed tomography angiography (CTA) is widely used to detect CAD, the morphology of coronary artery stenosis does not always cause a corresponding myocardial perfusion abnormality [3,4]. Recent developments in computed tomography (CT) technology have enabled CT perfusion (CTP) imaging [5–7], and dynamic CTP allows for a quantitative assessment of myocardial perfusion, which provides high diagnostic performance for detecting perfusion abnormalities [8–10].

The quantitative parameters of dynamic CTP (e.g., myocardial blood flow [MBF]) are obtained by analyzing the time attenuation curves (TAC) of the myocardium [11]. A high sampling rate on dynamic CTP is preferable to accurately assess the MBF, but it leads to an increase in the radiation dose. Several approaches have been applied to reduce the radiation dose of dynamic CTP; for instance, low-tube-voltage scanning and automated tube current modulation [12,13]. A low sampling rate of dynamic CTP has also been proposed for reducing radiation exposure in brain CTP imaging, but it might alter the hemodynamic parameters [14–16]. Currently, there is no consensus regarding the sampling rate for dynamic CTP of the myocardium, and the relationship between the sampling rate and robustness of CT-MBF has not been fully investigated in a clinical study.

* Corresponding author at: Department of Radiology, Ehime University Graduate School of Medicine, Shitsukawa, Toon City, Ehime 791-0295, Japan.
E-mail addresses: t.k.ehime@gmail.com (T. Kido), shikeda@m.ehime-u.ac.jp (S. Ikeda), izutani@m.ehime-u.ac.jp (H. Izutani), miyagawa@m.ehime-u.ac.jp (M. Miyagawa), tmochi@m.ehime-u.ac.jp (T. Mochizuki).

https://doi.org/10.1016/j.clinimag.2019.03.016
Received 23 October 2018; Received in revised form 23 March 2019; Accepted 29 March 2019

We aimed to estimate the influence of the sampling rate on dynamic CTP to quantify myocardial perfusion and the diagnostic performance when detecting myocardial perfusion abnormalities in a clinical setting.

2. Methods

The present retrospective study was approved by our institutional ethics committee. This study was registered in the Protocol Registration System of the UMIN Clinical Trials Registry (UMIN 000032605).

2.1. Study population

We collected data on 179 consecutive patients who underwent stress dynamic CTP for the assessment of CAD between July 2013 and November 2017. Among 179 patients, 47 underwent cardiac magnetic resonance (MR) imaging for the assessment of myocardial perfusion and viability. The indication for cardiac CT and MR imaging was determined by the attending physician at his or her discretion, based on clinical symptoms, initial cardiac examinations, and the pretest probability of CAD.

Patients were excluded if they had any of the following: (1) acute myocardial infarction (< 30 days from the onset), (2) cardiomyopathy, (3) left ventricular ejection fraction < 20%, (4) atrial fibrillation, (5) an atrioventricular block greater than the first degree, (6) complete left bundle branch block, (7) history of percutaneous coronary intervention or coronary artery bypass grafting, (8) poor cardiac MR image quality, and (9) an inappropriate CTP dataset such as that with insufficient image quality, misaligned scan coverage, and delayed data acquisition of dynamic CTP causing a shorter baseline (before upslope) of the TAC in the ascending aorta. The radiation dose was calculated from the dose-length product in a dose report (conversion factor = 0.014).

2.2. Cardiac CT: scanning protocol

A combined scanning protocol of stress dynamic CTP and coronary CTA was used according to a previously reported method [10]. A 256-slice multi-detector row CT unit (Brilliance iCT, Philips Healthcare, Cleveland, OH, USA), an automatic dual injector (Stellant DualFlow, Nihon Medrad KK, Osaka, Japan), and high-concentration contrast medium ([CM], iopamidol 370 mg iodine/mL; Bayer Yakuhin, Ltd., Osaka, Japan) were used. A timing bolus with a 20% diluted CM (5.0 mL/s for 10 s) and saline chaser (5.0 mL/s for 4 s) was administered. The delay time of the dynamic CTP was determined as 6 s before contrast enhancement in the ascending aorta to ensure that the baseline TAC had been achieved. After 3 min of adenosine triphosphate (ATP) infusion (Adetphos-L Kowa injection 20 mg; Kowa Inc., Tokyo, Japan; 0.16 mg/kg/min for 5 min), dynamic CTP was performed for 30 consecutive heartbeats in the prospective electrocardiogram-gated scan mode at a target phase of 40% of the RR interval (end-systolic phase) using a CM (5.0 mL/s for 10 s) and saline chaser (5.0 mL/s for 4 s). Subsequently, coronary CTA was performed. The scanning parameters for dynamic CTP were gantry rotation speed, 0.27 s/rotation; detector collimation, 64 × 1.25 mm; tube voltage, 100 kV; and tube current-time product, 80 mAs.

2.3. Post-processing of dynamic CTP images

Dynamic CTP images with a 3-mm slice thickness were reconstructed with filtered-back projection and a 360° reconstruction algorithm. The original dataset of dynamic CTP consisted of 30 cardiac phases with 1:1 heartbeat (1RR) sampling data acquisition. In this study, three additional CTP datasets were generated from the original data by selecting acquisition data at every other, every third, and every fourth heartbeat (1:2 [2RR], 1:3 [3RR], and 1:4 [4RR] sampling, respectively) (Fig. 1A). The CTP datasets were post-processed with elastic registration (for motion compensation) and a spatio-diffusion filter (to reduce image noise spikes over time) using a dedicated workstation (IntelliSpace Portal, Philips Healthcare). One radiologist, with 7 years of experience using cardiac CT, blindly analyzed the CT-MBF images using a dedicated workstation (Synapse Vincent, Fuji Medical Systems, Tokyo, Japan). The CT-MBF calculation was based on deconvolution analysis [10]. The left ventricular global and segmental CT-MBFs of the four different CTP datasets (sampling rates: 1RR, 2RR, 3RR, and 4RR) were automatically calculated on the voxel basis and presented as mean values with a polar map using a 16-segment model, excluding the apex [17] (Fig. 1B).

2.4. Cardiac MR: protocol and image analysis

The comprehensive cardiac MR imaging protocol consisted of stress/rest MR myocardial perfusion imaging (MR-MPI) and late gadolinium enhancement (LGE) imaging as previously described [18]. A 3 T MR imaging system (Achieva 3.0 T Quasar Dual; Philips Healthcare, Best, The Netherlands) that was equipped with a 32-element cardiac phased-array coil was used. Stress and rest dynamic MR-MPI was performed during and 10 min after ATP infusion (0.16 mg/min/kg for 3 min). Data for every cardiac cycle were acquired for 35 s after a bolus injection of a gadolinium-based CM (0.1 mmol/kg gadopentetate dimeglumine, Magnevist; Schering, Germany; injection rate, 4 mL/s) and saline chaser (30 mL, 4 mL/s). The perfusion sequence was acquired in three identical short-axis locations (basal, mid, and apical left ventricles) using a two-dimensional T1 turbo field-echo sequence with the k-space and time broad-use linear acquisition speed-up technique (k-t BLAST). The imaging parameters were as follows: repetition time, 3.7 ms; echo time, 1.85 ms; flip angle, 20°; section thickness, 8 mm; field of view, 400 mm; matrix size, 256 × 179; and k-t BLAST factor, 5. LGE images were obtained with an inversion-recovery three-dimensional T1 turbo field-echo sequence at 10 min after rest dynamic MR-MPI. The LGE imaging parameters were as follows: repetition time, 3.5 ms; echo time, 1.69 ms; inversion time, 400–500 ms (adjusted to the null signal of the normal myocardium using the Look Locker sequence); flip angle, 15°; section thickness, 6 mm; field of view, 350 mm; matrix size, 224 × 157; and sensitivity encoding (SENSE) reduction factor, 2.

Two experienced radiologists (with 9 and 13 years of cardiac MR experience) visually analyzed all MR images in a blinded fashion. Using the 16-segment model that excluded the apex [17], the radiologists classified the myocardial segments into three groups: (i) normal segment: normal perfusion observed on both stress and rest images and LGE not present; (ii) ischemic segment: a perfusion defect observed on a stress image, normal perfusion observed on a rest image, and no LGE; or (iii) infarcted segment: perfusion defects observed on stress/rest images and LGE was present. Myocardial segments with ischemia or infarction were defined as MR-MPI abnormalities. In case of disagreement between the radiologists, a final diagnosis was reached by consensus.

2.5. Statistical analyses

All data are expressed as the mean ± standard deviation or median (interquartile range), as appropriate. The paired *t*-test was used to compare the blood pressure (BP), or the heart rate (HR), before and during the ATP injection. The global CT-MBFs with 2RR, 3RR, and 4RR sampling were compared to that with 1RR sampling as a reference, using the two one-sided test of equivalence for paired-samples (TOST-P) with Bonferroni's correction [19–22]. The equivalence boundaries were determined within ± 5% of the mean CT-MBF value of the original data (1RR sampling). The Pearson rank correlation test was used to assess the relationship between the global CT-MBF with 1RR sampling and that with 2RR, 3RR, or 4RR sampling. To perform a sub-analysis, all patients were divided into two subgroups based on the HR during CTP scan: 1) high HR subgroup, patients with HR of > 75 beats/min (60 patients); and 2) low HR subgroup, patients with HR of 75 beats/min or less (60 patients). The TOST-P with Bonferroni's correction was used to

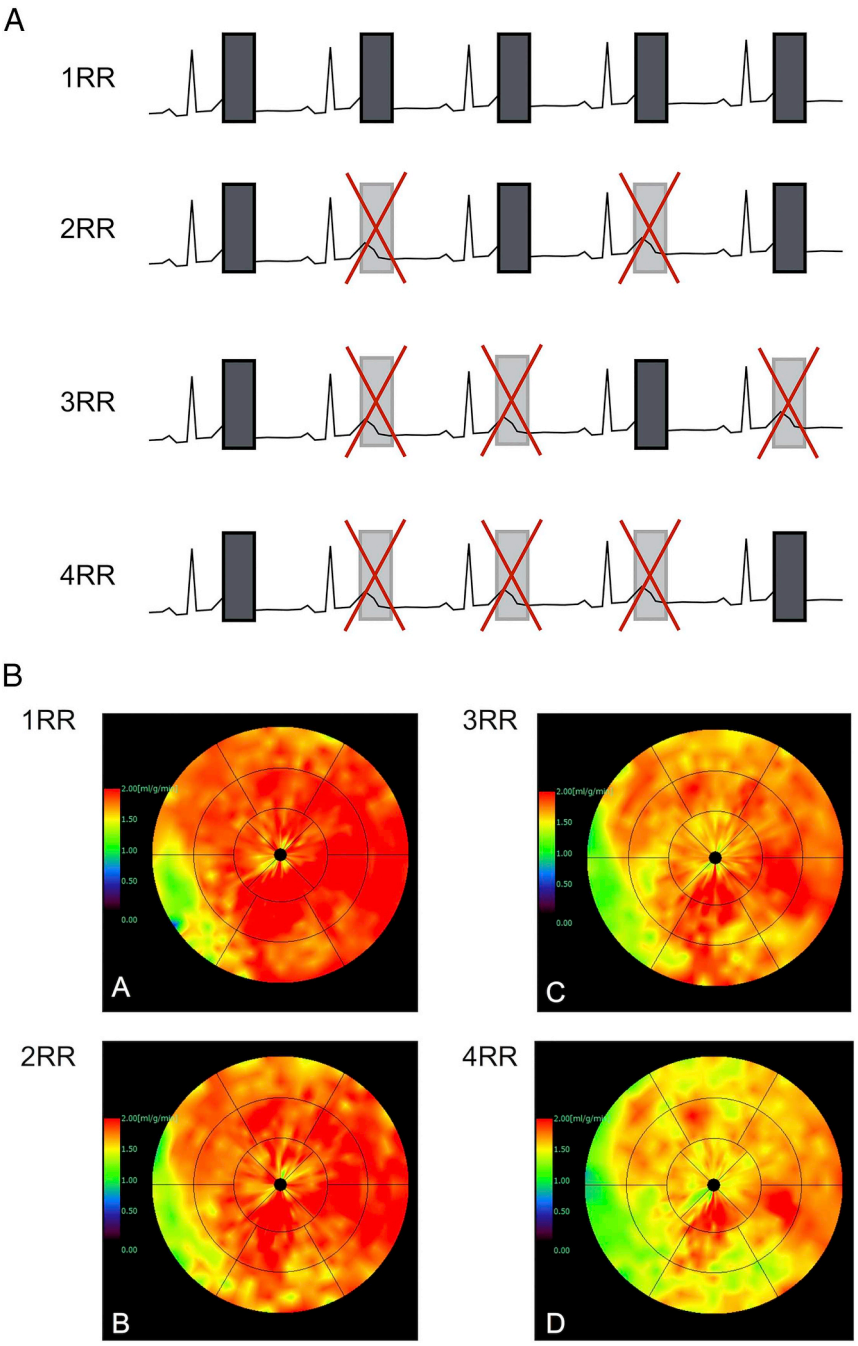

Fig. 1. Assumption of the sampling rate for dynamic CTP.
(A) Original dynamic CTP was acquired at a sampling rate of 1RR interval of the cardiac cycle. Three additional CTP datasets were created from the original dataset by selecting every other (2RR), every third (3RR), and every fourth (4RR) sampling.
(B) The polar maps of CT-MBF that were derived from dynamic CTP with sampling rates of 1RR (A), 2RR (B), 3RR (C), and 4RR (D).
CTP: computed tomography perfusion; CT-MBF: computed tomography-derived myocardial blood flow; RR: R-peak to R-peak.

compare global CT-MBFs with 2RR, 3RR, and 4RR sampling to that with 1RR sampling for patients in high and low HR subgroups in the same manner as that of the equivalence boundaries. Cohen's κ-value was used to examine the inter-observer variability of the qualitative assessment of cardiac MR. The TOST-P with Bonferroni's correction was used to compare segmental CT-MBFs with 2RR, 3RR, and 4RR sampling to that with 1RR sampling for normal and abnormal myocardial segments assessed with cardiac MR in the same manner as that of the equivalence boundaries. The clustered nature of the data was adjusted using logistic generalized estimating equations for the CTP segment-based analysis [23]. A receiver operating characteristic curve analysis was used to calculate the area under the curve of segmental CT-MBF for detecting perfusion abnormalities on cardiac MR. The areas under the curve of segmental CT-MBF with 2RR, 3RR, and 4RR sampling were compared to that with 1RR sampling [24]. The cutoff values were determined using the Youden index [25]. The sensitivity, specificity, positive predictive values, and negative predictive values for detecting MR-MPI abnormalities were determined for each dynamic CTP dataset. In all tests, statistical significance was determined as $p < 0.05$. In the statistical analyses with Bonferroni's correction, the p-values were described with threefold value. When the threefold p-value exceeds 1.000, we described $p > 1.000$ as $p = 1.000$. The statistical analyses were

Table 1
Patient characteristics.

Number of patients	120
Age (years)	68.3 ± 10.0
Men	78 (65)
Body mass index (kg/m^2)	24.6 ± 3.9
Coronary risk factors	
Hypertension	77 (64)
Dyslipidemia	60 (50)
Diabetes mellitus	44 (37)
Positive smoking history	60 (50)
Family history of CAD	31 (26)
Heart rate (beats/min)	
Before ATP injection	63.7 ± 10.1
During ATP injection	78.2 ± 12.5

CAD: coronary artery disease; ATP: adenosine triphosphate.
Data are presented as a number (percentage) or mean ± standard deviation.

performed with JMP11 (SAS Institute, Cary, NC, USA) and the statistical program R version 3.2.4 (R Foundation for Statistical Computing, Vienna, Austria, http://cran.r-project.org).

3. Results

3.1. Study population

Of 179 patients, 59 were excluded due to incomplete dynamic CTP data acquisition for this study protocol (n = 36), a history of revascularization (n = 13), arrhythmia (n = 3), cardiomyopathy (n = 2), poor image quality on cardiac MR images (n = 2), insufficient image quality on CTP (n = 2), and misaligned scanning coverage on CTP (n = 1), respectively. Finally, 120 patients, including 32 who underwent cardiac MR imaging, were enrolled in the present study. The patients' characteristics are shown in Table 1. The 10-year CAD death pre-test probabilities were < 0.5% (n = 8), 0.5–1% (n = 13), 1–2% (n = 20), 2–5% (n = 36), 5–10% (n = 18), > 10% (n = 25), according to a risk assessment based on a 19-year follow-up study of Japanese representative population study (NIPPON DATA80) [26]. The BP significantly decreased during ATP loading (systolic BP: 167.1 ± 25.0 mm Hg versus [vs.] 153.2 ± 26.3 mm Hg, diastolic BP: 71.2 ± 11.5 mm Hg vs. 66.3 ± 11.5 mm Hg, $p < 0.05$ for each). The HR significantly increased during ATP loading (63.7 ± 10.1 beats/min vs. 78.2 ± 12.5 beats/min, $p < 0.05$). The HRs under the stress state in the high and low HR subgroups were 88.8 ± 9.4 beats/min and 68.1 ± 5.8 beats/min. The mean effective radiation doses were 10.5 ± 0.4 mSv and 6.6 ± 5.3 mSv for CTP and coronary CTA, respectively. In the 32 patients who underwent cardiac MR imaging, the median interval between stress dynamic CTP and cardiac MR imaging was 28 days (12–42 days). No patient presented with worsening angina or cardiac events such as hospitalization for revascularization therapy or heart failure during the imaging session.

3.2. Equivalences and relationships of global CT-MBF according to the sampling rate

The estimation of the global CT-MBF is shown in Table 2. The global CT-MBFs with 1RR, 2RR, 3RR, and 4RR sampling were 1.57 ± 0.34 mL/g/min, 1.54 ± 0.35 mL/g/min, 1.51 ± 0.37 mL/g/min, and 1.41 ± 0.33 mL/g/min, respectively.

The global CT-MBF with 2RR sampling was significantly equivalent to that with 1RR ($p < 0.05$). Significant correlations in the global CT-MBF were seen between 1RR sampling and 2RR, 3RR, or 4RR ($p < 0.05$ for each; r = 0.91 for 1RR vs. 2RR, r = 0.89 for 1RR vs. 3RR, and r = 0.82 for 1RR vs. 4RR) (Fig. 2A–C). The estimation of the global CT-MBF in the high and low HR subgroups is also shown in Table 2. In the high HR subgroup, the global CT-MBFs 1RR, 2RR, 3RR, and 4RR sampling were 1.74 ± 0.32 mL/g/min, 1.72 ± 0.35 mL/g/min, 1.69 ± 0.38 mL/g/min, and 1.56 ± 0.35 mL/g/min, respectively. Significant equivalence was seen between 1RR sampling and 2RR sampling ($p < 0.05$). In the low HR subgroup, the global CT-MBFs 1RR, 2RR, 3RR, and 4RR sampling were 1.40 ± 0.27 mL/g/min, 1.37 ± 0.28 mL/g/min, 1.32 ± 0.25 mL/g/min, and 1.27 ± 0.25 mL/g/min, respectively. Significant equivalence was not observed in each pair.

Table 2
Estimation of the global CT-MBF for the sampling rate.

	CT-MBF (mL/g/min)	Difference from 1RR (%)	*p*-Value
All patients			
1RR sampling	1.57 ± 0.34		
2RR sampling	1.54 ± 0.36	−2.0 (−3.7 to −0.3)	< 0.001
3RR sampling	1.51 ± 0.37	−4.3 (−6.2 to −2.3)	0.699
4RR sampling	1.41 ± 0.33	−10.2 (−12.5 to −7.9)	1.000
High HR group			
1RR sampling	1.74 ± 0.32		
2RR sampling	1.72 ± 0.35	−1.5 (−3.8 to 0.8)	0.004
3RR sampling	1.69 ± 0.38	−2.8 (−5.5 to −0.2)	0.159
4RR sampling	1.56 ± 0.35	−10.7 (−13.9 to −7.4)	1.000
Low HR group			
1RR sampling	1.40 ± 0.27		
2RR sampling	1.37 ± 0.28	−2.6 (−5.2 to −0.07)	0.110
3RR sampling	1.32 ± 0.25	−6.1 (−9.0 to −3.2)	1.000
4RR sampling	1.27 ± 0.25	−9.5 (−12.8 to −6.3)	1.000

CT-MBF: computed tomography myocardial blood flow; 1RR: 1:1 heartbeat; 2RR: 1:2 heartbeat; 3RR: 1:3 heartbeat; 4RR: 1:4 heartbeat; HR: heart rate. The CT-MBF values are expressed as the mean ± standard deviation. The percentage of the differences in the CT-MBF value with 1RR sampling and 2RR, 3RR, or 4RR sampling to the mean CT-MBF value of 1RR sampling dataset are expressed as the mean (95% confidence interval). Note that the *p*-values are described with threefold values adjusted by Bonferroni's correction. The *p*-value is described it as $p = 1.000$, when the threefold *p*-value exceeds 1.000. $^*p < 0.05$ indicates statistically significant equivalence between the CT-MBF for each sampling rate and 1RR sampling.

3.3. Diagnostic performance of segmental CT-MBF for the detection of myocardial perfusion abnormalities, depending on the sampling rate

A total of 512 segments (in 32 patients) were assessed with cardiac MR imaging, and the myocardium was classified as normal in 274 segments (54%), ischemic in 196 (38%), and infarcted in 42 (8%). Finally, 238 segments were classified as myocardial segments with MR-MPI abnormalities. The inter-observer agreement for the qualitative assessment of cardiac MR was 0.86, which indicated satisfactory reliability ($\kappa > 0.70$).

The estimation of segmental CT-MBF is shown in Table 3. In normal myocardial segments, the mean values of segmental CT-MBF with 1RR, 2RR, 3RR, and 4RR sampling were 1.64 ± 0.33 mL/g/min, 1.59 ± 0.32 mL/g/min, 1.53 ± 0.36 mL/g/min, and 1.43 ± 0.33 mL/g/min, respectively. Significant equivalence was seen between 1RR sampling and 2RR sampling ($p < 0.05$) (Fig. 3A). In ischemic myocardial segments, the mean values of segmental CT-MBF with 1RR, 2RR, 3RR, and 4RR sampling were 1.27 ± 0.31 mL/g/min, 1.26 ± 0.30 mL/g/min, 1.23 ± 0.31 mL/g/min, and 1.21 ± 0.34 mL/g/min, respectively. Significant equivalence was observed between 1RR sampling and 2RR or 3RR sampling ($p < 0.05$ for each) (Fig. 3B). In infarcted myocardial segments, the mean values of segmental CT-MBF with 1RR, 2RR, 3RR, and 4RR sampling were 1.02 ± 0.22 mL/g/min, 1.02 ± 0.24 mL/g/min, 1.02 ± 0.24 mL/g/min, and 0.98 ± 0.31 mL/g/min, respectively. Significant equivalence was observed between 1RR sampling and 2RR or 3RR sampling ($p < 0.05$ for each) (Fig. 3C).

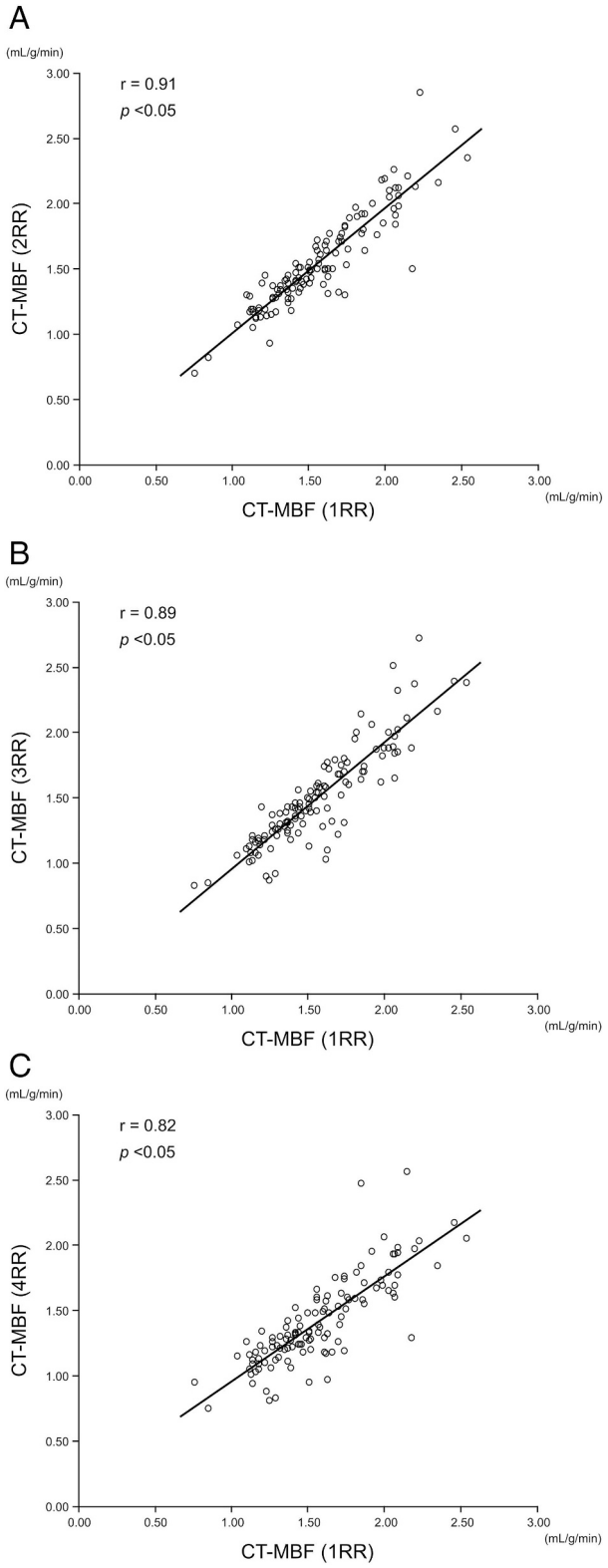

Fig. 2. Estimation of correlations in the global CT-MBF between 1RR (original data set) and the assumed lower sampling.
Correlations (r) were 0.91, 0.89, and 0.82 for 1RR vs. 2RR sampling (A), 1RR vs. 3RR sampling (B), and 1RR vs. 4RR (C), respectively.
CT-MBF: computed tomography-derived myocardial blood flow; RR: R-peak to R-peak; vs.: versus.

Table 3
Estimation of segmental CT-MBF for the sampling rate.

	CT-MBF (mL/g/min)	Difference from 1RR (%)	*p*-Value
Normal segments			
1RR sampling	1.64 ± 0.33		
2RR sampling	1.59 ± 0.32	−3.0 (−4.0 to −2.0)	< 0.001
3RR sampling	1.53 ± 0.36	−6.8 (−8.6 to −5.1)	1.000
4RR sampling	1.43 ± 0.33	−12.7 (−14.6 to −10.9)	1.000
Ischemic segments			
1RR sampling	1.27 ± 0.31		
2RR sampling	1.26 ± 0.30	−1.1 (−2.4 to 0.2)	< 0.001
3RR sampling	1.23 ± 0.31	−3.1 (−4.7 to −1.4)	0.035
4RR sampling	1.21 ± 0.34	−5.0 (−7.4 to −2.7)	1.000
Infarcted segments			
1RR sampling	1.02 ± 0.22		
2RR sampling	1.02 ± 0.24	0.02 (−2.6 to 2.6)	< 0.001
3RR sampling	1.02 ± 0.24	−0.02 (−4.1 to 4.1)	0.028
4RR sampling	0.98 ± 0.31	−4.4 (−11.9 to −3.2)	1.000

CT-MBF: computed tomography myocardial blood flow; 1RR: 1:1 heartbeat; 2RR: 1:2 heartbeat; 3RR: 1:3 heartbeat; 4RR: 1:4 heartbeat. The CT-MBF values are expressed as the mean ± standard deviation. The percentage of the differences in the CT-MBF value with 1RR sampling and 2RR, 3RR, or 4RR sampling to the mean CT-MBF value of 1RR sampling dataset are expressed as the mean (95% confidence interval). Note that the *p*-values are described with threefold values adjusted by Bonferroni's correction. The *p*-value is described it as $p = 1.000$, when the threefold *p*-value exceeds 1.000. $*p < 0.05$ indicates statistically significant equivalence among the CT-MBFs for each sampling rate compared with the 1RR sampling as a reference.

According to the receiver operating characteristic curve analysis, the areas under the curve of segmental CT-MBF with 1RR, 2RR, 3RR, and 4RR sampling for detecting perfusion abnormalities on cardiac MR were 0.84 (95% confidence interval [CI]: 0.80–0.88), 0.83 (95% CI: 0.79–0.86), 0.79 (95% CI: 0.75–0.83), and 0.76 (95% CI: 0.72–0.80), respectively (Table 4). A significant difference in the area under the curve of segmental CT-MBF was seen between 1RR sampling and 3RR or 4RR sampling ($p < 0.05$ for each). The sensitivity, specificity, positive predictive value, and negative predictive value of segmental CT-MBF for each sampling rate are shown in Table 4. Representative patients with myocardial ischemia (Fig. 4) and infarction (Fig. 5) show that the effects of sampling rate to CT-MBF quantification.

4. Discussion

The main findings of this study were as follows: (1) global CT-MBF with 2RR sampling is equivalent to that with 1RR sampling; (2) reduced sampling influenced the CT-MBF calculation, especially in a normal myocardium; and (3) 3RR and greater sampling of dynamic CTP impaired the diagnostic performance for detecting myocardial perfusion abnormalities.

The quantification of dynamic myocardial CTP is influenced by the temporal resolution of dynamic CTP data depending on the sampling rate and HR during scanning. Although a sampling of every heartbeat is theoretically desirable to obtain the optimal CTP data to quantify myocardial perfusion [27], this is not always feasible, and therefore, several sampling rates have been applied in previous clinical studies [8–10,28]. In the present study, global CT-MBF with 2RR sampling was significantly equivalent to that with 1RR sampling as a reference, while CT-MBF with 3RR or 4RR sampling was not. The mean value of global CT-MBF was reduced and the correlation with reference (1RR sampling) was weakened as sampling rate decreased (Table 2, Fig. 2). Ishida et al. reported that reduced sampling of a dynamic scan led to an

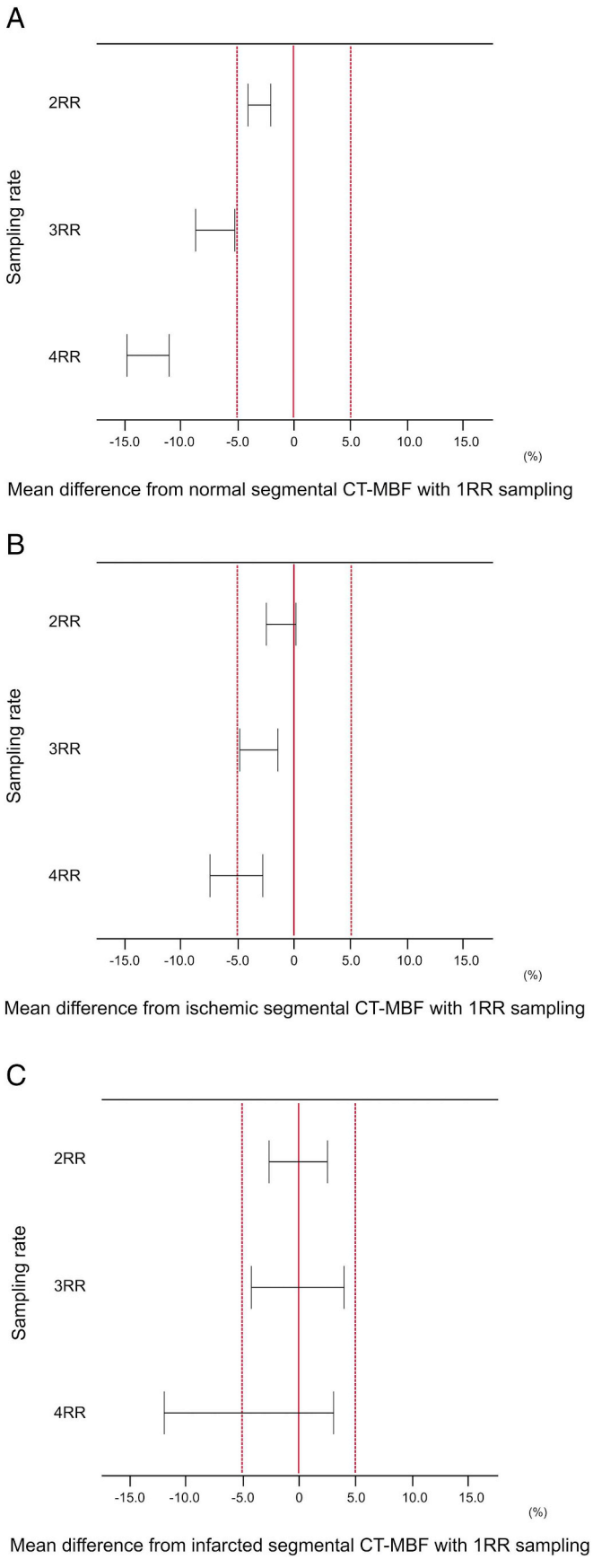

Fig. 3. Estimation of equivalences in segmental CT-MBF between 1RR and the assumed lower sampling.
Error bars indicate the 95% confidence interval of the mean percentage of difference between segmental CT-MBF with 1RR sampling and that with 2RR, 3RR, or 4RR sampling to the mean CT-MBF value of the 1RR sampling dataset. (A) A significant equivalence is observed between 1RR and 2RR sampling in normal myocardial segments. The equivalence boundary (red dotted lines) was determined at 5% of the mean CT-MBF value of the 1RR sampling dataset (−5%, 5%). (B) Significant equivalencies are observed between 1RR and 2RR sampling and 1RR and 3RR sampling in ischemic myocardial segments. The equivalence boundary (red dotted lines) was determined at 5% of the mean CT-MBF value of the 1RR sampling dataset (−5%, 5%). (C) Significant equivalencies are observed between 1RR and 2RR sampling and 1RR and 3RR sampling in infarcted myocardial segments. The equivalence boundary (red dotted lines) was determined at 5% of the mean CT-MBF value of the 1RR sampling dataset (−5%, 5%).
CT-MBF: computed tomography-derived myocardial blood flow; RR: R-peak to R-peak. (For interpretation of the references to color in this figure legend, the reader is referred to the web version of this article.)

underestimation of the quantitative parameters of myocardial perfusion in a simulation study [29]. Modgil et al. indicated that precise data acquisition around the delivery time of CM (the starting point of TAC) and peak enhancement time of the myocardium (the peak point of TAC) were important factors for accurately computing MBF [30], and reduced sampling of dynamic CTP led to the risk of overlooking the start or peak point of TAC.

The present study showed that reduced sampling had a greater influence on the CT-MBF calculation in high HR groups than in low HR groups (Table 2). The interval time of scan in a low HR patient is longer than in a high HR patient. Therefore, the low HR group might be more sensitive to a reduced sampling rate.

The present study showed that reduced sampling had a greater influence on the CT-MBF calculation in normal myocardium than in abnormal myocardium (Table 3, Fig. 3). This is because MBF in normal myocardium is substantially greater than that in abnormal myocardium under stress and has higher temporal frequency information in TAC than abnormal myocardium, and a higher sampling rate is necessary to acquire accurate perfusion data from a normal myocardium than in an abnormal myocardium [31]. Therefore, reduced sampling of a perfusion scan may have a major impact on a normal myocardium, which might reduce the differences in CT-MBF between normal and abnormal myocardia. Accordingly, the diagnostic performance of CT-MBF for detecting myocardial perfusion abnormalities was impaired by reduced sampling of dynamic CTP (Table 4).

The stress MBF values in normal myocardium observed in the previous CT studies are substantially smaller than MBF values obtained by the gold standard method, such as Oxygen-15-labelled water positron emission tomography (PET) by several factors such as the uptake kinetics of contrast medium, acquisition protocols, and post-processing methods [10,32]. Thus, the cut-off values of stress MBF for the detection of significant CAD determined in the CT studies are different from that in perfusion PET study.

Our study showed that 2RR sampling was equivalent to 1RR sampling for global CT-MBF and segmental CT-MBF in normal and abnormal myocardia, and there was no significant difference in the diagnostic performance of CT-MBF with 1RR and 2RR sampling for detecting myocardial perfusion abnormalities. Huber et al. also showed that CT-MBF with 2RR sampling had high diagnostic performance for detecting obstructive CAD as a reference of the fractional flow reserve [28]. The present results indicated that dynamic CTP with reduced sampling of the 2RR interval would be useful for reducing the radiation dose (e.g. 15/30 phases for 2RR sampling = 50% reduction) and maintaining diagnostic performance.

Although the CT-MBF values obtained from 2RR to 4RR sampling showed significant correlation with the CT-MBF values obtained from

Table 4
Diagnostic performance of CT-MBF for detecting MR-MPI abnormalities according to the sampling rate.

Sampling rate	AUC	*p*-Value	Cutoff value (mL/g/min)	Sensitivity (%)	Specificity (%)	PPV (%)	NPV (%)
1RR	0.84 (0.80–0.88)	–	1.41	82 (76–86)	84 (80–88)	81 (78–86)	84 (80–88)
2RR	0.83 (0.79–0.86)	0.149	1.40	79 (71–86)	78 (71–85)	76 (71–82)	81 (77–86)
3RR	0.79 (0.75–0.83)	< 0.001	1.36	77 (72–87)	73 (62–79)	72 (66–76)	79 (75–86)
4RR	0.76 (0.72–0.80)	< 0.001	1.30	78 (69–87)	69 (58–79)	69 (64–75)	78 (73–85)

CT-MBF: computed tomography-derived myocardial blood flow; MR-MPI: magnetic resonance myocardial perfusion imaging; AUC: area under the curve; PPV: positive predictive value; NPV: negative predictive value; 1RR: 1:1 heartbeat; 2RR: 1:2 heartbeat, 3RR: 1:3 heartbeat, 4RR: 1:4 heartbeat. Data are expressed as a percentage (95% confidence interval). Note that the *p*-values are described with threefold values adjusted by Bonferroni's correction. The *p*-value is described it as $p = 1.000$, when the threefold *p*-value exceeds 1.000. *$p < 0.05$ indicates the statistical significance of the AUC value, compared with a sampling rate of 1RR.

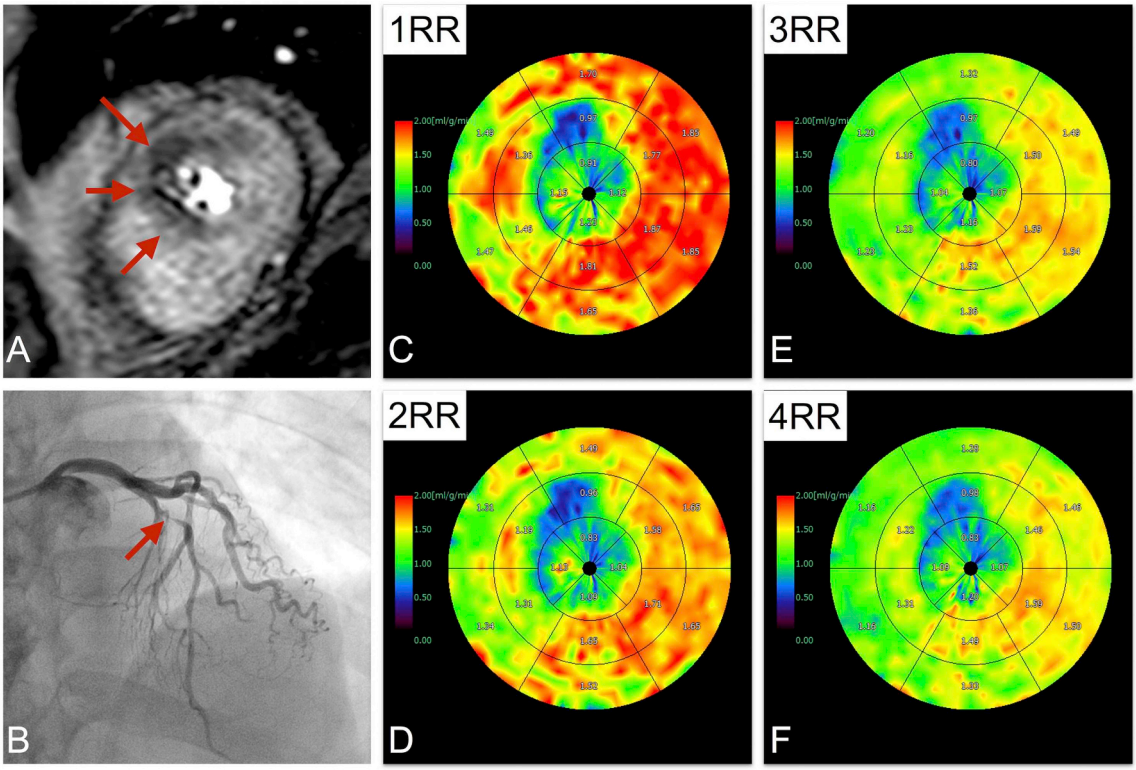

Fig. 4. A 61-year-old man with effort angina.
Stress MR-MPI shows a perfusion defect (red arrows) in the antero-septal area of the left ventricle in an apical image (A). Coronary angiography shows severe stenosis (red arrow) in the mid-portion of the left anterior descending artery (B). A polar map of CT-MBF with 1RR sampling (original data set) clearly reveals lower CT-MBF in the same area from the mid-portion to the apex of the left anterior descending artery (C). Polar maps of CT-MBF with 2RR (D), 3RR (E), and 4RR (F) sampling show that a lower sampling rate attenuated the differences in CT-MBF between normal and abnormal myocardia by reduced sampling on a dynamic CTP scan.
MR-MPI: magnetic resonance myocardial perfusion imaging; CT-MBF: computed tomography-derived myocardial blood flow; RR: R-peak to R-peak. (For interpretation of the references to color in this figure legend, the reader is referred to the web version of this article.)

1RR sampling in this study, the correlation coefficients were lower in order from 2RR to 4RR sampling because several factors such as scan HR and true MBF affected the influence of reducing sampling rate on the quantification of CT-MBF. Hence, we speculated that linear regression may be insufficient to accurately correct the CT-MBF obtained from low sampling rate. Hubbard et al. reported the feasibility of calculation method of true MBF from CTP data with low sampling rate in animal study [33]. Further investigation is required to establish the accurate calculation method of true MBF from CTP data with low sampling rate in clinical study. Moreover, Tomizawa et al. reported that the CT-MBF with low sampling rate provided the incremental value over diagnostic performance of coronary CTA alone in combination with myocardial segmentation using Voronoi method and relative CT-MBF ratio [34]. These reinforcements also have a possibility to improve the diagnostic performance of CT-MBF with low sampling rate.

This study has several limitations. First, this was a retrospective cohort study with a small population. A larger prospective study is necessary. Second, we could not compare CT-MBF with other MPI modalities such as PET, which has been established as the gold standard [35,36]. Third, the CT-MBFs obtained in this study were relatively lower than those obtained by PET studies as mentioned above [32]. Finally, we used only a single calculation formula that was based on model-independent deconvolution. A further study using other calculation methods such as the maximum slope method, two-compartment model, and others is required.

In conclusion, our study demonstrates that dynamic myocardial CTP with 2RR sampling is feasible for the quantification of CT-MBF based on deconvolution analysis, providing similar performance as that of 1RR sampling while reducing radiation dose. Further reductions to the

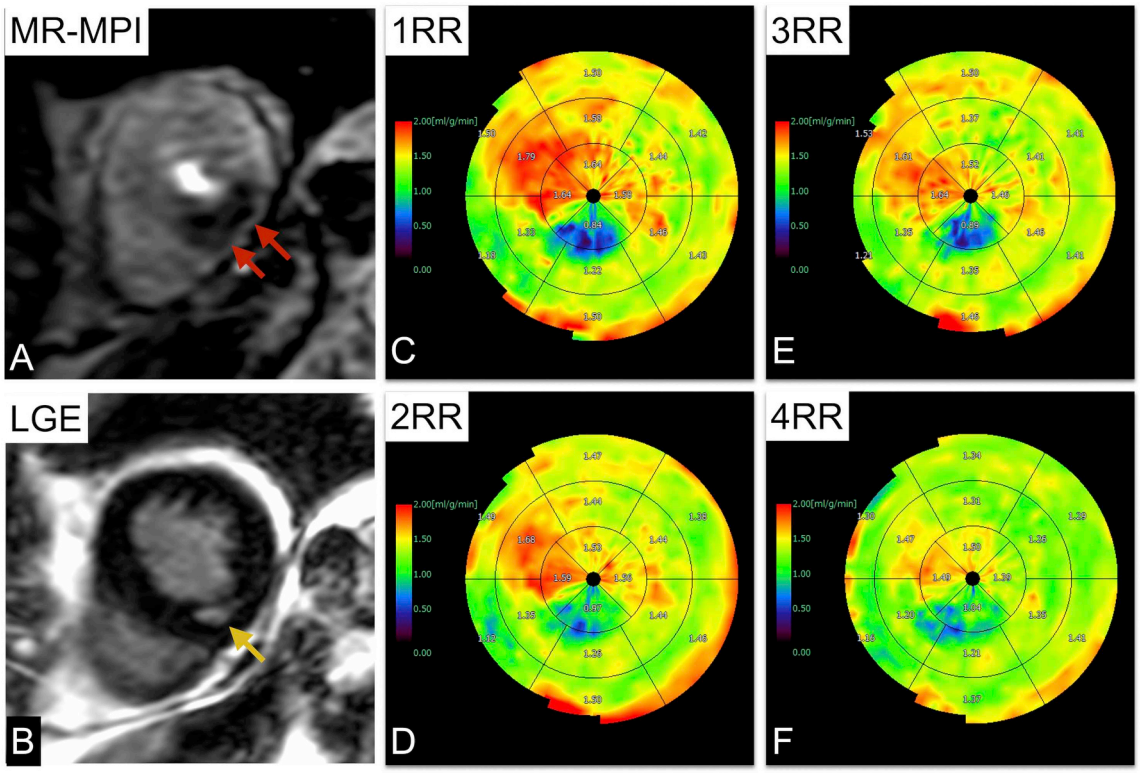

Fig. 5. A 73-year-old woman with myocardial infarction.
Stress MR-MPI shows a perfusion defect (red arrows) in the apical inferior area (A). Late image shows subendocardial infarction as late gadolinium enhancement in a part (yellow arrow) of the same area (B). The polar map of CT-MBF with 1RR sampling (original data set) reveals lower CT-MBF in the same area (C). Polar maps of CT-MBF with 2RR (D), 3RR (E), and 4RR (F) sampling show that a lower sampling rate attenuated the differences in CT-MBF between normal and abnormal myocardia by reduced sampling on a dynamic CTP scan.
MR-MPI: magnetic resonance myocardial perfusion imaging; CT-MBF: computed tomography-derived myocardial blood flow; RR: R-peak to R-peak. (For interpretation of the references to color in this figure legend, the reader is referred to the web version of this article.)

sampling rate affect the CT-MBF calculation, thereby impairing the diagnostic performance for detecting myocardial perfusion abnormalities.

Conflicts of interest

None.

Acknowledgements

We appreciate Kenta Yamada (Fujifilm Co., Ltd., Tokyo, Japan), Jun Masumoto (Fujifilm Co., Ltd., Tokyo, Japan), Shinichi Tokuyasu (Philips Japan, Tokyo, Japan), and Mani Vembar (Philips Healthcare, OH, USA) for valuable technical comments. We asked for a statistical review and advice for this manuscript from StaGen Co. Ltd.

Funding

This research did not receive any specific grant from funding agencies in the public, commercial, or not-for-profit sectors.

References

[1] Hachamovitch R, Di Carli MF. Methods and limitations of assessing new non-invasive tests: part II: outcomes-based validation and reliability assessment of noninvasive testing. Circulation 2008;117:2793–801. https://doi.org/10.1161/CIRCULATIONAHA.107.714006.

[2] Shaw LJ, Berman DS, Maron DJ, Mancini GB, Hayes SW, Hartigan PM, et al. Optimal medical therapy with or without percutaneous coronary intervention to reduce ischemic burden: results from the Clinical Outcomes Utilizing Revascularization and Aggressive Drug Evaluation (COURAGE) trial nuclear substudy. Circulation 2008; 117: 1283–91. doi:https://doi.org/10.1161/CIRCULATIONAHA.107.743963.

[3] Schuijf JD, Wijns W, Jukema JW, Atsma DE, de Roos A, Lamb HJ, et al. Relationship between noninvasive coronary angiography with multi-slice computed tomography and myocardial perfusion imaging. J Am Coll Cardiol 2006; 48: 2508–14. doi:https://doi.org/10.1016/j.jacc.2006.05.080.

[4] Meijboom WB, Van Mieghem CA, van Pelt N, Weustink A, Pugliese F, Mollet NR, et al. Comprehensive assessment of coronary artery stenoses: computed tomography coronary angiography versus conventional coronary angiography and correlation with fractional flow reserve in patients with stable angina. J Am Coll Cardiol 2008;52:636–43. https://doi.org/10.1016/j.jacc.2008.05.024.

[5] Cury RC, Magalhães TA, Borges AC, Shiozaki AA, Lemos PA, Júnior JS, et al. Dipyridamole stress and rest myocardial perfusion by 64-detector row computed tomography in patients with suspected coronary artery disease. Am J Cardiol 2010; 106: 310–5. doi:https://doi.org/10.1016/j.amjcard.2010.03.025.

[6] Bettencourt N, Chiribiri A, Schuster A, Ferreira N, Sampaio F, Pires-Morais G, et al. Direct comparison of cardiac magnetic resonance and multi detector computed tomography stress-rest perfusion imaging for detection of coronary artery disease. J Am Coll Cardiol 2013;61:1099–107. https://doi.org/10.1016/j.jacc.2012.12.020.

[7] Rochitte CE, George RT, Chen MY, Arbab-Zadeh A, Dewey M, Miller JM, et al. Computed tomography angiography and perfusion to assess coronary artery stenosis causing perfusion defects by single photon emission computed tomography: the CORE320 study. Eur Heart J 2014; 35: 1120–30. doi:https://doi.org/10.1093/eurheartj/eht488.

[8] Ho KT, Chua KC, Klotz E, Panknin C. Stress and rest dynamic myocardial perfusion imaging by evaluation of complete time-attenuation curves with dual-source CT. JACC Cardiovasc Imaging 2010;3:811–20. https://doi.org/10.1016/j.jcmg.2010.05.009.

[9] Bamberg F, Marcus RP, Becker A, Hildebrandt K, Bauner K, Schwarz F, et al. Dynamic myocardial CT perfusion imaging for evaluation of myocardial ischemia as determined by MR imaging. JACC Cardiovasc Imaging 2014; 7: 267–77. doi:https://doi.org/10.1016/j.jcmg.2013.06.008.

[10] Tanabe Y, Kido T, Uetani T, Kurata A, Kono T, Ogimoto A, et al. Differentiation of myocardial ischemia and infarction assessed by dynamic computed tomography perfusion imaging and comparison with cardiac magnetic resonance and single-photon emission computed tomography. Eur Radiol 2016; 26: 3790–801. doi:https://doi.org/10.1007/s00330-016-4238-1.

[11] George RT, Jerosch-Herold M, Silva C, Kitagawa K, Bluemke DA, Lima JA, et al. Quantification of myocardial perfusion using dynamic 64-detector computed

tomography. Invest Radiol 2007; 42: 815–22. doi:https://doi.org/10.1097/RLI.0b013e318124a884.
[12] Patel AR, Lodato JA, Chandra S, Kachenoura N, Ahmad H, Freed BH, et al. Detection of myocardial perfusion abnormalities using ultra-low radiation dose regadenoson stress multidetector computed tomography. J Cardiovasc Comput Tomogr 2011; 5: 247–54. doi:https://doi.org/10.1016/j.jcct.2011.06.004.
[13] Kim SM, Kim YN, Choe YH. Adenosine-stress dynamic myocardial perfusion imaging using 128-slice dual-source CT: optimization of the CT protocol to reduce the radiation dose. Int J Cardiovasc Imaging 2013;29:875–84. https://doi.org/10.1007/s10554-012-0138-x.
[14] Wiesmann M, Berg S, Bohner G, Klingebiel R, Schöpf V, Stoeckelhuber BM, et al. Dose reduction in dynamic perfusion CT of the brain: effects of the scan frequency on measurements of cerebral blood flow, cerebral blood volume, and mean transit time. Eur Radiol 2008;18:2967–74. doi:https://doi.org/10.1007/s00330-008-1083-x.
[15] Wintermark M, Smith WS, Ko NU, Quist M, Schnyder P, Dillon WP. Dynamic perfusion CT: optimizing the temporal resolution and contrast volume for calculation of perfusion CT parameters in stroke patients. AJNR Am J Neuroradiol 2004;25:720–9.
[16] Kämena A, Streitparth F, Grieser C, Lehmkuhl L, Jamil B, Wojtal K, et al. Dynamic perfusion CT: optimizing the temporal resolution for the calculation of perfusion CT parameters in stroke patients. Eur J Radiol 2007;64:111–18. doi:https://doi.org/10.1016/j.ejrad.2007.02.025.
[17] Cerqueira MD, Weissman NJ, Dilsizian V, Jacobs AK, Kaul S, Laskey WK, et al. American Heart Association Writing Group on Myocardial Segmentation and Registration for Cardiac Imaging. Standardized myocardial segmentation and nomenclature for tomographic imaging of the heart. A statement for healthcare professionals from the Cardiac Imaging Committee of the Council on Clinical Cardiology of the American Heart Association. Circulation 2002;105:539–42. https://doi.org/10.1016/j.cmpb.2008.03.002.
[18] Kido T, Nagao M, Kido T, Kurata A, Miyagawa M, Ogimoto A, et al. Stress/rest circumferential strain in non-ischemia, ischemia, and infarction–quantification by 3 Tesla tagged magnetic resonance imaging. Circ J 2013;77:1235–41.
[19] Schuirmann DL. On hypothesis testing to determine if the mean of a normal distribution is contained in a known interval. Biometrics 1981;37:617.
[20] Robinson AP, Froese RE. Model validation using equivalence tests. Ecol Model 2004;176:349–58.
[21] Wellek S. Testing statistical hypotheses of equivalence. United Kingdom: Chapman and Hall/CRC; 2003. p. 284.
[22] Westlake WJ. Response to T.B.L. Kirkwood: bioequivalence testing - a need to rethink. Biometrics 1981;37:589–94.
[23] Sternberg MR, Hadgu A. A GEE approach to estimating sensitivity and specificity and coverage properties of the confidence intervals. Stat Med 2001;20:1529–39.
[24] Zhou XH, Obuchowski NA, McClish DK. Statistical methods in diagnostic medicine. New York: John Wiley & Sons; 2002. p. 153–4.
[25] Perkins NJ, Schisterman EF. The inconsistency of “optimal” cutpoints obtained using two criteria based on the receiver operating characteristic curve. Am J Epidemiol 2006;163:670–5. https://doi.org/10.1093/aje/kwj063.
[26] NIPPON DATA80 Research Group. Risk assessment chart for death from cardiovascular disease based on a 19-year follow-up study of a Japanese representative population. Circ J 2006;70:1249–55.
[27] Rossi A, Merkus D, Klotz E, Mollet N, de Feyter PJ, Krestin GP. Stress myocardial perfusion: imaging with multidetector CT. Radiology 2014;70:25–46. https://doi.org/10.1148/radiol.13112739.
[28] Huber AM, Leber V, Gramer BM, Muenzel D, Leber A, Rieber J, et al. Myocardium: dynamic versus single-shot CT perfusion imaging. Radiology 2013;269:378–86. doi:https://doi.org/10.1148/radiol.13121441.
[29] Ishida M, Kitagawa K, Ichihara T, Natsume T, Nakayama R, Nagasawa N, et al. Underestimation of myocardial blood flow by dynamic perfusion CT: explanations by two-compartment model analysis and limited temporal sampling of dynamic CT. J Cardiovasc Comput Tomogr 2016;10:207–14. doi:https://doi.org/10.1016/j.jcct.2016.01.008.
[30] Modgil D, Bindschadler MD, Alessio AM, La Rivière PJ. Variable temporal sampling and tube current modulation for myocardial blood flow estimation from dose-reduced dynamic computed tomography. J Med Imaging (Bellingham) 2017;4:026002https://doi.org/10.1117/1.JMI.4.2.026002.
[31] Di Carli M, Czernin J, Hoh CK, Gerbaudo VH, Brunken RC, Huang SC, et al. Relation among stenosis severity, myocardial blood flow, and flow reserve in patients with coronary artery disease. Circulation 1995;91:1944–51.
[32] Kajander SA, Joutsiniemi E, Saraste M, Pietilä M, Ukkonen H, Saraste A, et al. Clinical value of absolute quantification of myocardial perfusion with (15)O-water in coronary artery disease. Circ Cardiovasc Imaging 2011;4:678–84. doi:https://doi.org/10.1161/CIRCIMAGING.110.960732.
[33] Hubbard L, Ziemer B, Lipinski J, Sadeghi B, Javan H, Groves EM, et al. Functional assessment of coronary artery disease using whole-heart dynamic computed tomographic perfusion. Circ Cardiovasc Imaging 2016;9. doi:https://doi.org/10.1161/CIRCIMAGING.116.005325.
[34] Tomizawa N, Chou S, Fujino Y, Kamitani M, Yamamoto K, Inoh S, et al. Feasibility of dynamic myocardial CT perfusion using single-source 64-row CT. J Cardiovasc Comput Tomogr 2019;13:55–61. doi:https://doi.org/10.1016/j.jcct.2018.10.003.
[35] Kaufmann PA, Gnecchi-Ruscone T, Yap JT, Rimoldi O, Camici PG. Assessment of the reproducibility of baseline and hyperemic myocardial blood flow measurements with 15O-labeled water and PET. J Nucl Med 1999;40:1848–56.
[36] Camici PG, Crea F. Coronary microvascular dysfunction. N Engl J Med 2007;356:830–40. https://doi.org/10.1056/NEJMra061889.